Supplementary Figure 1. Fatty acids accumulate more in crypt cells than in the villus cells. (A) Quantification of uptake of BODIPY^{TM} FL C16 (fluorescent palmitic acid). (B) Crypt and villus epithelial cells were isolated from duodenum, jejunum and ileum, and incubated with 10 μM BODIPY^{TM} FL C12 (red fluorescent dodecanoic acid) for 30 min. Scale bar, 50 μm. (C) Quantification of uptake of 2-NBDG (fluorescent glucose analog). ImageJ was used for fluorescence quantification. Data are presented as mean ± SEM (n=3 independent experiments, 3-6 representative images for each time points, Student's t-test, two-sided at $P < 0.01$** and$P < 0.05$*).

Supplementary Figure 2. HNF4 paralogs directly bind to and activate FAO genes. (A) Examples of HNF4 regulation of genes related to fatty acid β-oxidation. ChIP-seq tracks (n=2 biological replicates) show that HNF4 factors bind to FAO genes, and loss of HNF4 results in reduced H3K27ac signal or inaccessible chromatin (see black dashed rectangles). RNA-seq tracks (n=3 biological replicates) show that FAO genes are downregulated in *Hnf4αγ*^{DKO} compared to their littermate controls. (B) Summary schematic of results (n=3 biological replicates, 2-3 days post tamoxifen-induced knockout): loss of HNF4 factors results in downregulation of fatty acid β-oxidation (genes in blue color) and upregulation of fatty acid synthesis and lipogenesis (genes in red color).

Supplementary Figure 3. Glycolysis-pyruvate oxidation pathway-related genes are not compromised upon HNF4 loss. (A) Transcriptome analysis (n=3 biological replicates) shows elevated expression of glycolysis/pyruvate oxidation-related genes in *Hnf4αγ*^{DKO} (Statistical tests were embedded in Cuffdiff. Black color: significant genes with FDR < 0.05; Gray color: non-significant genes). (B) Schematic of glycolysis-pyruvate oxidation pathway. (C) Transcript levels related to pyruvate oxidation (PDH genes) are not compromised upon HNF4 loss. Statistical tests were embedded in Cuffdiff at FDR < 0.01** (n=3 biological replicates, 2-3 days post tamoxifen-induced knockout).

Supplementary Figure 4. Loss of HNF4 paralogs in the intestinal epithelium leads to stem cell loss. (A) Western blot shows complete loss of HNF4 in intestinal epithelial cells of *Hnf4αγ*^{DKO} (n=3 independent experiments, cells were collected 4 days after the first tamoxifen injection). Immunostaining of (B) OLFM4 (stem cell marker) and (C) GFP corroborates loss of stem cells. Red arrows indicate position of Lgr5-GFP^{+} stem cells in the control mice (representative of 3 biological replicates). (D) Quantification of the number of crypts that have HNF4A-null cells in **Fig. 3G**. Crypts showing at least 3 HNF4-null cells were considered to harbor HNF4A-negative cells, and 100 crypts were counted per biological replicate. Data are presented as mean ± SEM (Student's t-test, two-sided at $P < 0.001$*** and $P < 0.01$**). (E) Crypts lacking HNF4 factors are unable to form organoids. Crypts were harvested from *Hnf4αγ*^{DKO} after 2 days of tamoxifen injection (n=2 independent experiments). (F) Tamoxifen-induced Cre controls were also tested in the organoid culture assay (n=2 independent experiments).

Supplementary Figure 5. HNF4 may promote intestinal stem cell renewal via metabolic regulation. (A) 24 hours of U-$^{13}C_{16}$ palmitate (0.5 mM) labeling shows compromised ^{13}C labeled TCA metabolites in *Hnf4αγ*^{DKO} organoids (n=4 independent organoid cultures, expanded panel from **Fig. 5C**). (B) 6 hours of U-$^{13}C_2$ acetate (2.5 mM) labeling shows reduced TCA metabolite pool sizes upon HNF4 loss (n=4 independent organoid cultures). For all the ^{13}C tracer experiments, 1 μM tamoxifen was added to culture medium of primary organoids on Day 3 after seeding for 12 hours. All the organoids were harvested for LC-MS metabolite determination on Day 6. U-$^{13}C_{16}$ palmitate (24 hours) or U-$^{13}C_2$ acetate (6 hours) was added to the culture medium prior to harvesting. (C-D) Inhibition of FAO accelerates the formation of spherical organoids in *Hnf4αγ*^{DKO}. (C) Representative spherical morphology and (D) percentage of spherical organoid formation of *Hnf4αγ*^{DKO} with or without Etomoxir treatment (n=3

independent organoid cultures). 1 μM tamoxifen was added to culture medium of primary organoids on Day 2 after seeding. After 12 hours treatment with tamoxifen, Etomoxir was added to the culture medium. Untreated *Hnf4αγ*^{DKO} organoids show more buds than the treated group (see arrows). (E-G) The high levels of acetate and DCA can rescue *Hnf4αγ*^{DKO}, but seem to impair WT organoids. (E) Representative morphology (n=4 independent experiments). Scale bars, 50 μm. qRT-PCR shows compromised Lgr5^{+} stem cell markers in the WT organoids upon (F) 25 mM acetate treatment (n=3 independent organoid cultures) or (G) 10 mM DCA treatment (n=4 independent organoid cultures). Data are presented as mean ± SEM (Student's t-test, two-sided at $P < 0.001$***, $P < 0.01$** and $P < 0.05$*). Scale bars, 50 μm.

Fig. S1

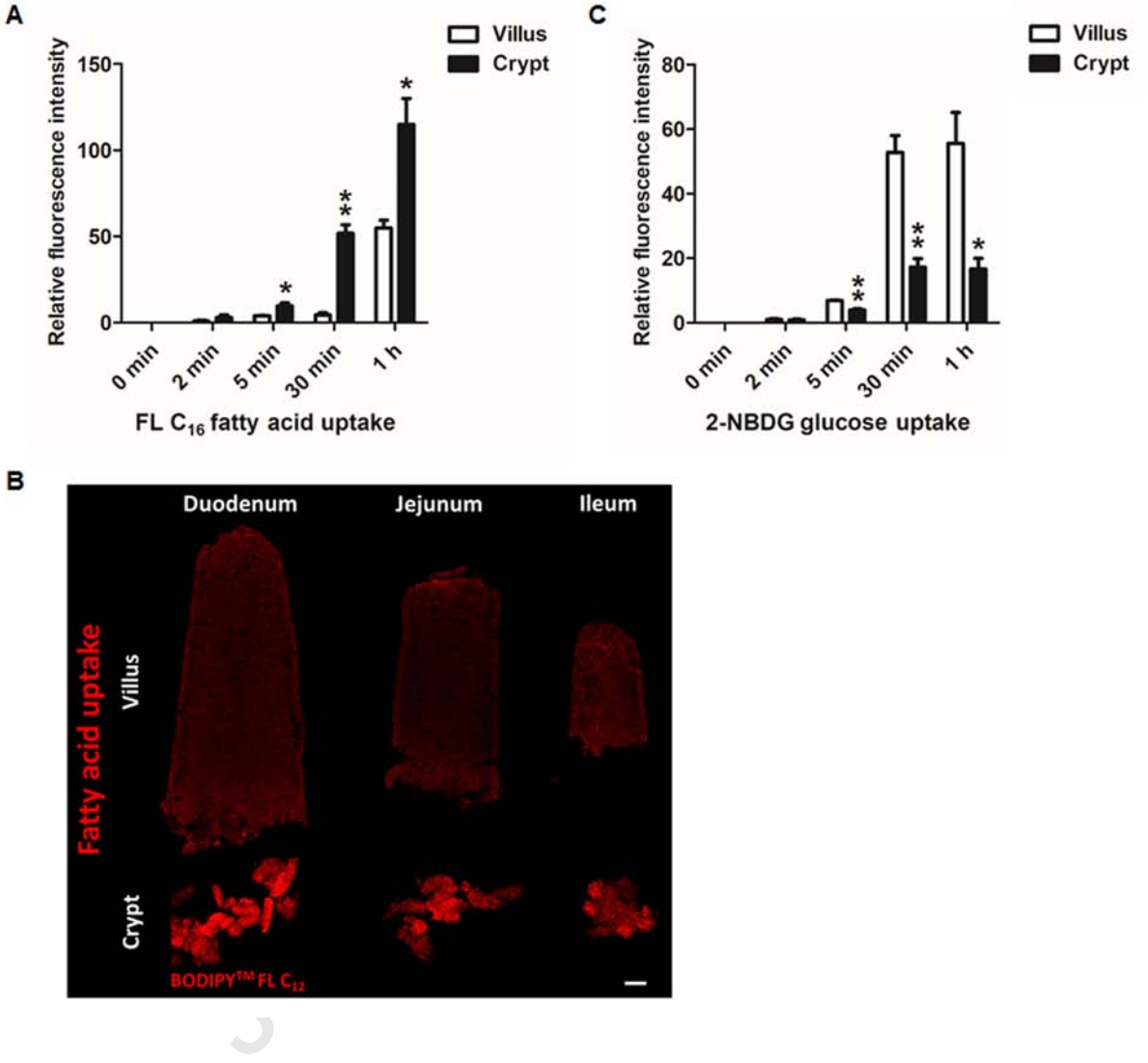
A
Villus
Crypt
Relative fluorescence intensity
150
100
50
0
0 min
2 min
5 min
30 min
1 h
FL C16 fatty acid uptake
C
Villus
Crypt
Relative fluorescence intensity
80
60
40
20
0
0 min
2 min
5 min
30 min
1 h
2-NBDG glucose uptake
B
Duodenum
Jejunum
Ileum
Fatty acid uptake
Villus
Crypt
BODIPY™ FL C12

Fig. S2

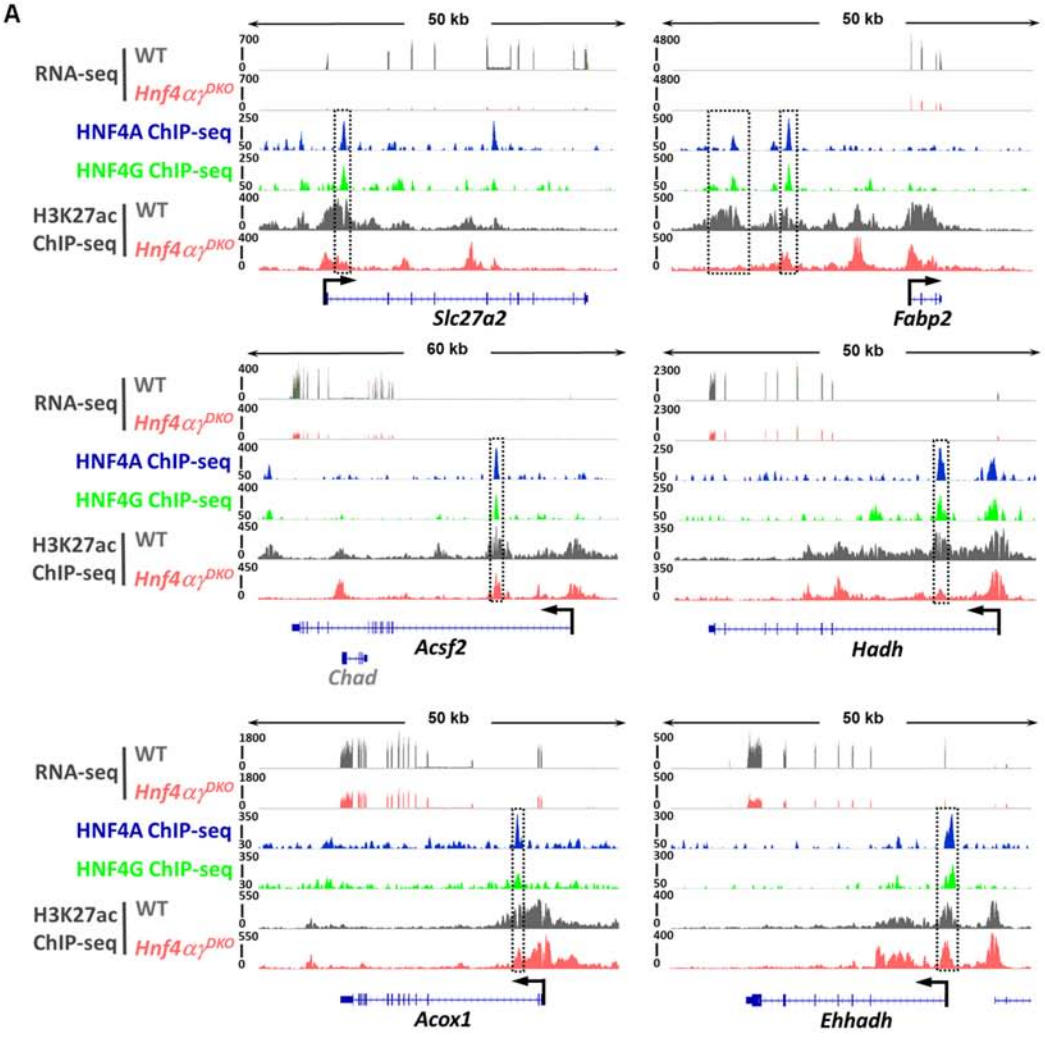
A
RNA-seq
WT
Hnf4αγDKO
HNF4A ChIP-seq
HNF4G ChIP-seq
H3K27ac ChIP-seq
50 kb
60 kb
Slc27a2
Fabp2
Acsf2
Chad
Hadh
Acox1
Ehhadh

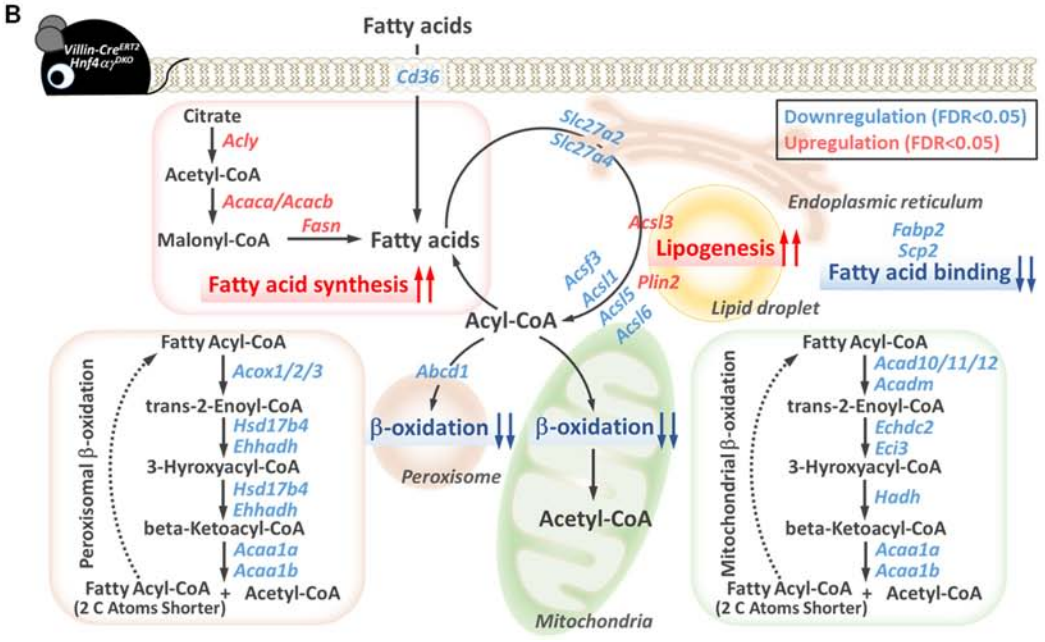
B
Villin-CreERT2 Hnf4αγDKO
Fatty acids
Cd36
Citrate
Acly
Acetyl-CoA
Acaca/Acacb
Malonyl-CoA
Fasn
Fatty acids
Fatty acid synthesis
Slc27a2
Slc27a4
Acsl3
Acsf3
Acsl1
Acsl5
Acsl6
Plin2
Acyl-CoA
Lipogenesis
Endoplasmic reticulum
Fabp2
Scp2
Fatty acid binding
Lipid droplet
Downregulation (FDR<0.05)
Upregulation (FDR<0.05)
Abcd1
β-oxidation
Peroxisome
Acetyl-CoA
Mitochondria
Fatty Acyl-CoA
Acox1/2/3
trans-2-Enoyl-CoA
Hsd17b4
Ehhadh
3-Hyroxyacyl-CoA
Hsd17b4
Ehhadh
beta-Ketoacyl-CoA
Acaa1a
Acaa1b
Fatty Acyl-CoA + Acetyl-CoA
(2 C Atoms Shorter)
Peroxisomal β-oxidation
Acad10/11/12
Acadm
Echdc2
Eci3
Hadh
Mitochondrial β-oxidation

Fig. S3

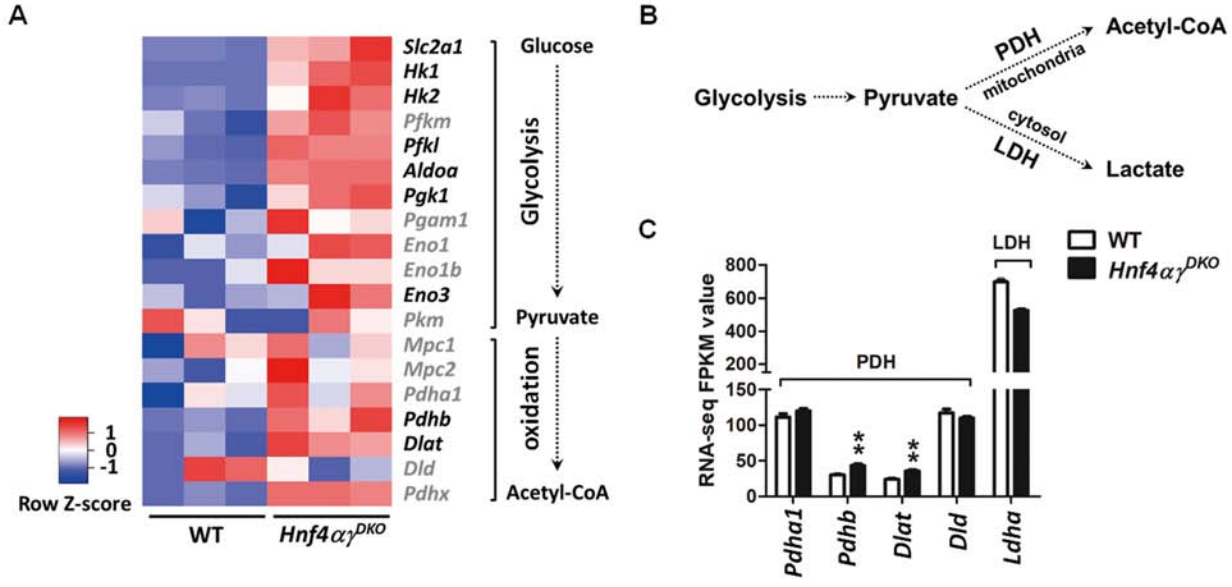

Fig. S4

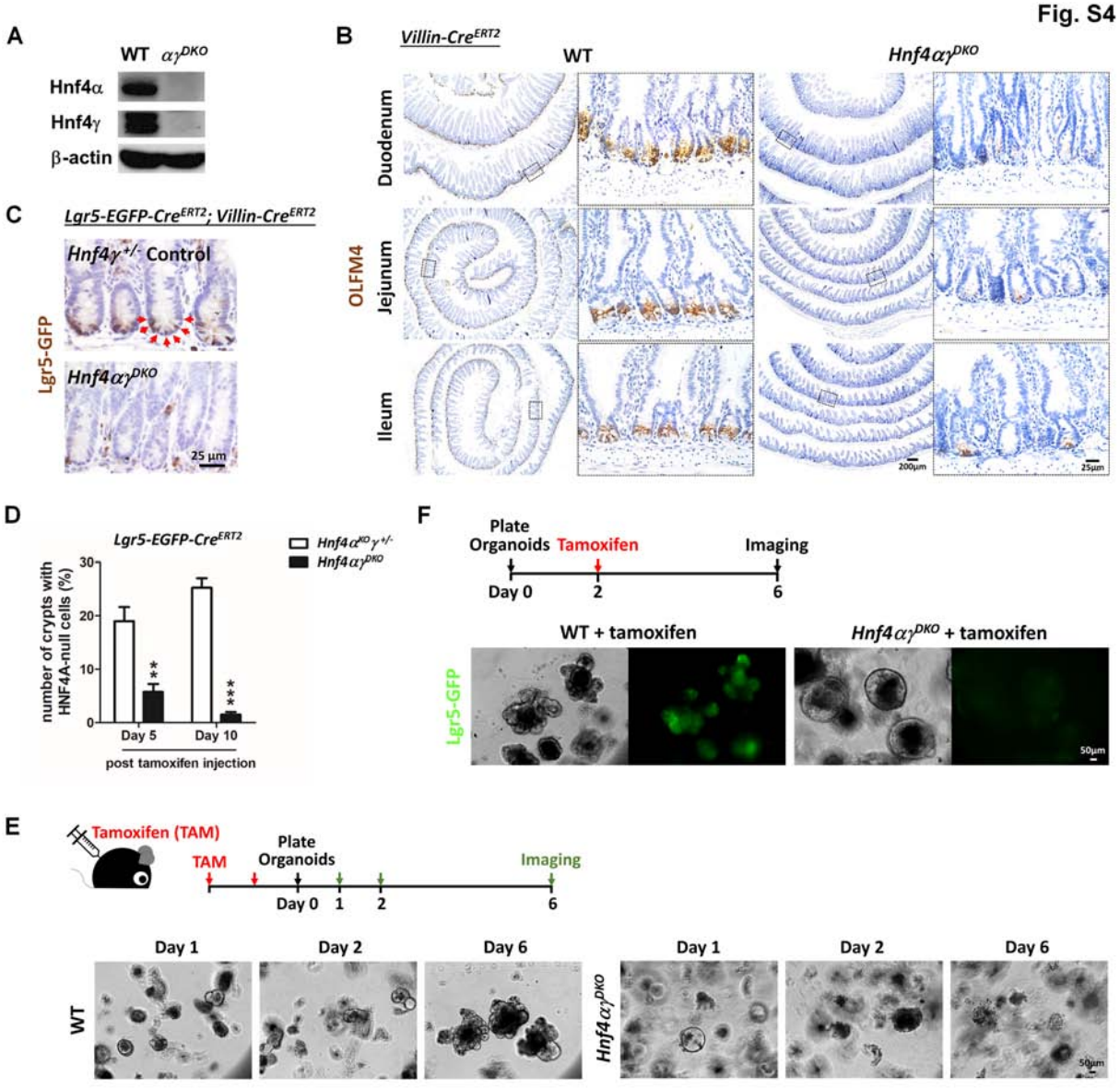
A
WT
αγDKO
Hnf4α
Hnf4γ
β-actin
B
Villin-CreERT2
WT
Hnf4αγDKO
Duodenum
Jejunum
Ileum
OLFM4
200μm
25μm
C
Lgr5-EGFP-CreERT2; Villin-CreERT2
Hnf4γ+/- Control
Hnf4αγDKO
Lgr5-GFP
25 μm
D
Lgr5-EGFP-CreERT2
Hnf4αKOγ+/-
Hnf4αγDKO
number of crypts with HNF4A-null cells (%)
30
20
10
0
**
***
Day 5
Day 10
post tamoxifen injection
F
Plate Organoids
Tamoxifen
Imaging
Day 0
2
6
WT + tamoxifen
Hnf4αγDKO + tamoxifen
Lgr5-GFP
50μm
E
Tamoxifen (TAM)
TAM
Plate Organoids
Imaging
Day 0
1
2
6
Day 1
Day 2
Day 6
WT
Hnf4αγDKO
50μm

Fig. S5

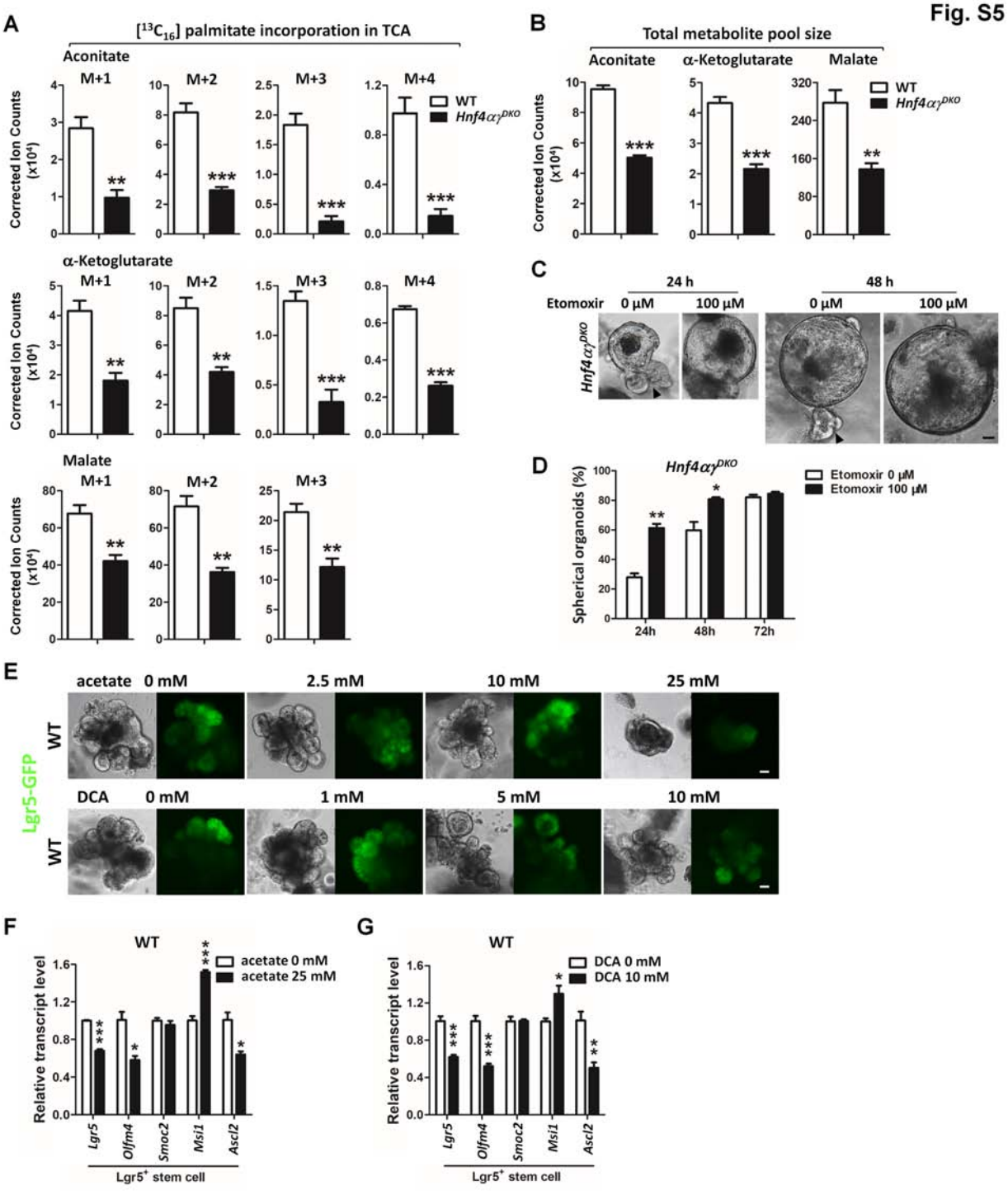
A
[13C16] palmitate incorporation in TCA
Aconitate
M+1
M+2
M+3
M+4
WT
Hnf4αγDKO
Corrected Ion Counts (x10⁴)
α-Ketoglutarate
Malate
B
Total metabolite pool size
Aconitate
α-Ketoglutarate
Malate
C
24 h
48 h
Etomoxir
0 μM
100 μM
Hnf4αγDKO
D
Hnf4αγDKO
Etomoxir 0 μM
Etomoxir 100 μM
Spherical organoids (%)
24h
48h
72h
E
acetate
0 mM
2.5 mM
10 mM
25 mM
DCA
1 mM
5 mM
WT
Lgr5-GFP
F
WT
acetate 0 mM
acetate 25 mM
Relative transcript level
Lgr5
Olfm4
Smoc2
Msi1
Ascl2
Lgr5+ stem cell
G
WT
DCA 0 mM
DCA 10 mM
Relative transcript level
Lgr5+ stem cell

Cell isolation of intestinal epithelium, villi and crypts

Freshly harvested mouse intestine was flushed with cold PBS, opened longitudinally, cut into 1 cm pieces, and then rotated in 3 mM EDTA in PBS at 4 °C. The tissue was then vigorously shaken to release the epithelium from underlying muscular tissue, and the supernatant was collected as the whole epithelium fraction; villi were collected from the top of a 70-μm cell strainer while crypts passed through. Cells were pelleted by centrifugation at 170 g at 4 °C and then washed with cold PBS. Cells were used for fatty acid/glucose analog uptake and RNA/protein extraction described in later sections.

Histology and immunostaining

Intestinal tissues were fixed overnight in 4% paraformaldehyde at 4°C, and then washed with PBS. If there is no designation, histologic analysis were done after four consecutive days of tamoxifen treatment. For paraffin embedding, tissues were then dehydrated through ascending alcohols and processed with xylene prior to embedding. For cryo-embedding, tissues were then processed with 15% sucrose and 30% sucrose until tissues sunk prior to freeze in OCT compound (Tissue-Tek 4583). 5 μm thick paraffin sections were used for immunohistochemistry and immunofluorescence staining using standard procedures. 10 μm thick cryosections were used for Lgr5-GFP detection of mouse duodenal epithelium. Immunohistochemistry was performed using primary antibodies against Hnf4α (Santa Cruz sc-6556 X, 1:2000), Hnf4ɣ (Santa Cruz sc-6558 X, 1:2000), Olfm4 (Cell Signaling 39141, 1:2500), GFP (Santa Cruz sc-9996, 1:200), and Cleaved Caspase 3 (Cell Signaling 9661, 1:200). After employing secondary antibody and the Vectastain ABC HRP Kit (Vector Labs), slides were developed using 0.05% DAB (Amresco, #0430) and 0.015% hydrogen peroxide in 0.1 M Tris, and then counterstained with hematoxylin. The slides were mounted and viewed on a Nikon Eclipse E800 microscope. Images were photographed with a Retiga 1300 CCD (QImaging) camera and QCapture imaging software. A Zeiss Axiovert 200M fluorescence microscope was used for imaging the Lgr5-GFP fluorescence and the immunofluorescence staining of Ki67 (Abcam ab16667, 1:100) by using a Retiga-SRV CCD (QImaging). ImageJ and Adobe Photoshop were used to adjust contrast and brightness. When adjustments were made, they were applied uniformly for comparative images.

RNA extraction and quantitative reverse transcription polymerase chain reaction (qRT-PCR)

For tissues, cells were isolated from mouse duodenum as described above, and processed for RNA extraction using Trizol (Invitrogen) according to the manufacturer's instructions. For cultured organoids, QIAGEN RNeasy Micro Kit was used to extract RNA according to the manufacturer's instructions. cDNA was synthesized from total RNA with Oligo$(dT)_{20}$ primers using SuperScript III First-Strand Synthesis SuperMix (Invitrogen). qRT-PCR was performed to measure changes in mRNA expression using Applied Biosystems 7900HT Sequence Detection System. The sequences of the primers used are available upon request. Briefly, the qRT-PCR was carried out using Power SYBR® Green PCR Master Mix, and the amplification conditions were as follows: 50°C for 2 min, 95°C for 10 min, followed by 40 cycles of 95°C for 15s and 60°C for 1 min. *Hprt1* was used as an internal control. The $2^{-\Delta\Delta Ct}$ method was applied to calculate the fold change of relative transcript level.

Protein extraction and Western blot

The protein of duodenal epithelium or intestinal organoids was extracted with RIPA buffer (50 mM Tris-HCl pH 8.0, 150 mM NaCl, 1% NP-40, 0.5% Na-deoxycholate, 0.1% SDS, protease inhibitor cocktails, and phosphatase inhibitors). Four cycles and two cycles of Bioruptor sonication (30 s on and 30 s off) were used before and after rotating cells in lysis buffer at 4 °C for 30 min, respectively. Protein concentration was determined by Pierce BCA Protein Assay Kit

(Thermo). Immunodetection was performed using specific antibodies against HNF4A (Santa Cruz sc-6556 X, 1:1000), HNF4G (Santa Cruz sc-6558 X; 1:1000) and β-actin (Abcam ab8227, 1:5000).

Organoid culture

Primary crypt-derived organoids were isolated from duodenal epithelium and cultured in Cultrex® reduced growth factor basement membrane matrix, Type R1 (Trevigen) according to established methods[1]. Organoids with Lgr5-GFP were isolated and cultured from duodenal crypts of *Lgr5-EGFP-IRES-Cre^{ERT2};Villin-Cre^{ERT2};*WT and *Lgr5-EGFP-IRES-Cre^{ERT2};Villin-Cre^{ERT2};Hnf4α$^{f/f}$;Hnf4γ$^{Crispr/Crispr}$* mice. The organoids were treated with 1 μM tamoxifen dissolved in ethanol for 12 hours. Vehicle-treated organoids served as a control. Tamoxifen was added into culture medium of organoids on Day 2 or Day 3 after seeding. Etomoxir (Sigma E1905), acetate (Sigma S5636) and DCA (Tocris 2755) were prepared according to the supplier's instructions, and vehicle controls were used. Organoids were imaged using a Zeiss Axiovert 200M inverted fluorescence microscope with a Retiga-SRV CCD (QImaging).

Organoid counting

Organoids were collected at Day 8 after seeding for each passage, washed with basal culture medium (BCM), and then treated with TrpLE by gently pipetting up and down. After removal of matrigel and another wash with BCM, organoids were dissociated with pre-warmed Trypsin at 37°C for 3 min. Organoids were subsequently mixed and counted with a hemocytometer. The number of surviving cells at each passage were normalized with primary passage (starting cell number) and split ratio.

Organoid immunofluorescence

Organoids were cultured in 8 well chamber slides (MatTek). After 6 days of seeding, organoids were fixed, permeabilized, and stained as described[2]. Organoids were treated with 10 μM EdU 6 hours prior to fixation, and the Click-iT™ EdU Alexa Fluor™ 488 Imaging Kit (Invitrogen C10337) was used to perform the EdU staining according to the manufacturer's instructions. A Zeiss LSM 510 Meta confocal microscope was used for imaging the immunofluorescence staining of EdU and Ki67 (Abcam ab16667, 1:100) in organoids.

FAO activity assay

Crypt and villus cells were scraped and collected from proximal small intestine of *Hnf4*αγ^{DKO} mice (3 days post tamoxifen injection) and their littermate controls. FAO assay kit (E-141L, Biomedical research service center at UB) was used to measure β-oxidation activity according to the supplier's instructions with a slight modification in sample preparation. Briefly, cell pellets were suspended in cell lysis solution (100 μl per 10 mg tissues). Bioruptor sonication (30s on and 30s off, 3 cycles) was used before and after rotating cells in lysis buffer at 4°C for 5 min. Lysates were centrifuged for 5-8 min at maximal speed at 4°C three times. The supernatant was collected and incubated with control solution and reaction solution at 37°C for 1 hour as described by the manufacturer. 3% acetic acid was added to stop the reaction. Each sample was mixed by thoroughly pipetting up and down and then measured for absorbance at 492 nm. Protein concentration was determined by Pierce BCA Protein Assay Kit (Thermo), and was used to normalize the FAO activity.

Fatty acid extraction and saponification

SPLASH Lipidomix internal standard (IS, Avanti Polar Lipids 330707) was diluted into methanol at 10x, and 120 μl of cold methanol-IS was added to 10 mg of organoid pellets. 1.0 mm Zirconium Oxide beads (Next advance Zr0B10) were then added to samples. All the samples were placed in Bullet Blender Blue homogenizer (Next Advance) on speed 6 for 2 min. After homogenization, samples were then subjected to extraction with 400 μl of cold MTBE (Sigma 650560), followed

by vortexing and then shaking for 6 min at 4°C. 100 µl of H_2O (LC-MS grade) was added to samples, and then centrifuged at 14000 rpm for 2 min. 160 µl of supernatant was transferred into a clean tube, dried down, and then resuspended in 1 ml of 0.3 M KOH in 90% methanol (90:10 methanol:H_2O). Samples were then transferred to glass vials and placed into water bath at 80°C for saponification. After 1 hour of saponification, samples were cooled on ice and acidified by adding 100 µl formic acid. Samples were then subjected to extraction with 1 ml of hexane, twice. The saponified fatty acids in hexane (top layer) were transferred into a glass vial, dried down, and then dissolved in 1 ml of methanol/isopropanol mixture (1:1) for subsequent LC-MS analysis. Protein concentration was determined by Pierce BCA Protein Assay Kit (Thermo), and was used to normalize the corrected ion counts of labeled fatty acids.

LC-MS analysis

LC-MS analysis of the extracted metabolites was conducted on Q Exactive Plus Hybrid Quadrupole-Orbitrap mass spectrometer (Thermo Fisher Scientific) coupled to hydrophilic interaction chromatography. The Dionex UltiMate 3000 UHPLC system (Thermo Fisher Scientific) with Waters XBridge BEH Amide column (2.1mm × 150mm, 2.5µm particle size, 130Å pore size) coupled with a Waters XBridge BEH Amide XP VanGuard cartridge (2.1mm x 5mm, 2.5µm particle size, 130Å pore size) guard column was used for LC separation. The LC gradient is comprised of solvent A (95%:5% H_2O:acetonitrile with 20 mM ammonium acetate, 20 mM ammonium hydroxide, pH 9.4) and solvent B (20%:80% H_2O:acetonitrile with 20 mM ammonium acetate, 20 mM ammonium hydroxide, pH 9.4) in the following solvent B percentages over time: 0 min, 100%: 3 min, 100%; 3.2 min, 90%; 6.2 min, 90%; 6.5 min, 80%; 10.5 min, 80%; 10.7 min, 70%; 13.5 min, 70%; 13.7 min, 45%; 16 min, 45%; 16.5 min, 100%. Chromatography flow rate was at 300 µL/min and injection volume 5 µL. Column temperature was maintained at 25 °C. MS scans were set to negative ion mode with a resolution of 70,000 at m/z 200, in addition to an automatic gain control target of 3×10^6 and m/z scan range of 72 to 1000. Metabolite data was obtained using the MAVEN software package[3] with each labeled isotope fraction (mass accuracy window: 5 ppm). The isotope natural abundance and tracer isotopic impurity were corrected using AccuCor[4].

LC-MS analysis of the saponified fatty acids was conducted on Q Exactive Plus Hybrid Quadrupole-Orbitrap mass spectrometer (Thermo Fisher Scientific) coupled to reverse phase chromatography. The Dionex UltiMate 3000 UHPLC system (Thermo Fisher Scientific) with Poroshell 120 EC-C18 column (150 mm × 2.1 mm, 2.7 µM particle size, Agilent) was used for LC separation. The LC gradient is comprised of solvent A (90%:10% H2O:methanol with 1 mM ammonium acetate, 35 mM acetic acid), and solvent B (98%:2% isopropanol:methanol with 1 mM ammonium acetate, 35 mM acetic acid). The gradient was 0 min, 25% B; 2 min, 25% B; 5.5 min, 65% B; 9.5 min, 100% B; 13.5 min, 100% B; 14.5 min, 25% B; 20min, 25% B. Chromatography flow rate was at 200 µL/min and injection volume 5 µL. Column temperature was maintained at 45 °C. MS scans were set to negative ion mode with a resolution of 140,000 at m/z 200, in addition to an automatic gain control target of 3×10^6 and m/z scan range of 200 to 600. Metabolite data was obtained using the MAVEN software package[3] with each labeled isotope fraction (mass accuracy window: 5 ppm). The isotope natural abundance and tracer isotopic impurity were corrected using AccuCor[4].

Bioinformatics

For RNA-seq, raw sequencing reads (fastq) were quality checked with fastQC (v0.11.3) and were further aligned to mouse (mm9) genomes using Tophat2 (v2.1.0) to generate bam files. Cuffquant (v2.2.1) was used to generate cxb files from bam files. Cuffnorm (v2.2.1) was performed to calculate FPKM values using quartile normalization. Cuffdiff (v2.2.1)[5] was applied

to identify differentially expressed genes between the control and the mutants using quartile normalization and per-condition dispersion. Genes with FPKM > 1 were used for further analysis. Cuffdiff was used to generate the pre-ranked gene list. Gene set enrichment analysis (GSEA) was performed on the pre-ranked gene list as described[6]. Heatmapper[7] was used to display relative transcript levels of genes of interest by using normalized FPKM values from Cuffnorm. For ATAC-seq and ChIP-seq, fastQC (v0.11.3) was used to check the quality of raw sequencing reads (fastq), and bowtie2 (v2.2.6) was used to align the sequences to mouse (mm9) genome and generate bam files. Deeptools bamCoverage[8] (v2.4.2, duplicate reads ignored, RPKM normalized and extended reads) was used to generate bigwig files from bam files. BigWigMerge (UCSC) was used to merge the bigwig files of different replicates. The Integrative Genomics Viewer[9] (IGV) was used to visualize normalized bigwig tracks. Model-based Analysis of ChIP-Seq[10] (MACS 1.4.1) was used for peak calling and to generate bed files from aligned reads. For HNF4 ChIP-seq, the shiftsize parameter used in MACS was based on the fragment size of Pippin Prep. BEDTools[11] was used to merge the intervals of bed files. Homer findMotifsGenome.pl[12] (v4.8.3, homer *de novo* Results) was used to call transcription factor motifs enriched at peaks.

1. Sato T, Vries RG, Snippert HJ, et al. Single Lgr5 stem cells build crypt-villus structures in vitro without a mesenchymal niche. Nature 2009;459:262-5.
2. O'Rourke KP, Dow LE, Lowe SW. Immunofluorescent Staining of Mouse Intestinal Stem Cells. Bio Protoc 2016;6.
3. Melamud E, Vastag L, Rabinowitz JD. Metabolomic analysis and visualization engine for LC-MS data. Anal Chem 2010;82:9818-26.
4. Su X, Lu W, Rabinowitz JD. Metabolite Spectral Accuracy on Orbitraps. Anal Chem 2017;89:5940-5948.
5. Trapnell C, Roberts A, Goff L, et al. Differential gene and transcript expression analysis of RNA-seq experiments with TopHat and Cufflinks. Nat Protoc 2012;7:562-78.
6. Subramanian A, Tamayo P, Mootha VK, et al. Gene set enrichment analysis: a knowledge-based approach for interpreting genome-wide expression profiles. Proc Natl Acad Sci U S A 2005;102:15545-50.
7. Babicki S, Arndt D, Marcu A, et al. Heatmapper: web-enabled heat mapping for all. Nucleic Acids Res 2016;44:W147-53.
8. Ramirez F, Ryan DP, Gruning B, et al. deepTools2: a next generation web server for deep-sequencing data analysis. Nucleic Acids Res 2016;44:W160-5.
9. Robinson JT, Thorvaldsdottir H, Winckler W, et al. Integrative genomics viewer. Nat Biotechnol 2011;29:24-6.
10. Zhang Y, Liu T, Meyer CA, et al. Model-based analysis of ChIP-Seq (MACS). Genome Biol 2008;9:R137.
11. Quinlan AR. BEDTools: The Swiss-Army Tool for Genome Feature Analysis. Curr Protoc Bioinformatics 2014;47:11 12 1-34.
12. Heinz S, Benner C, Spann N, et al. Simple combinations of lineage-determining transcription factors prime cis-regulatory elements required for macrophage and B cell identities. Mol Cell 2010;38:576-89.